A Comparison of Absorption and Emission Line Abundances in the Nearby Damped Lyman-α Galaxy SBS 1543+593[1]

David V. Bowen[2], Edward B. Jenkins[2], Max Pettini[3], Todd M. Tripp[4]

[2] *Princeton University Observatory, Princeton, NJ 08544*

[3] *Institute of Astronomy, Madingley Rd., Cambridge CB3 0EZ, UK*

[4] *Dept. of Astronomy, University of Massachusetts, Amherst, MA 01003*

ABSTRACT

We have used the Space Telescope Imaging Spectrograph (STIS) aboard HST to measure a sulfur abundance of [S/H] = -0.41 ± 0.06 in the interstellar medium (ISM) of the nearby damped Lyman-α (DLA) absorbing galaxy SBS 1543+593. A direct comparison between this QSO absorption line abundance on the one hand, and abundances measured from H II region emission line diagnostics on the other, yield the same result: the abundance of sulfur in the neutral ISM is in good agreement with that of oxygen measured in an H II region 3 kpc away. Our result contrasts with those of other recent studies which have claimed order-of-magnitude differences between H I (absorption) and H II (emission) region abundances. We also derive a nickel abundance of [Ni/H] < -0.81, some three times less than that of sulfur, and suggest that the depletion is due to dust, although we cannot rule out an over-abundance of alpha-elements as the cause of the lower metallicity. It is possible that our measure of [S/H] is over-estimated if some S II arises in ionized gas; adopting a plausible star formation rate for the galaxy along the line of sight, and a measurement of the C II* λ1335.7 absorption line detected from SBS 1543+593, we determine that the metallicity is unlikely to be smaller than we derive by more than 0.25 dex. We estimate that the cooling rate of the cool neutral medium is $\log[l_c$ (ergs s^{-1} H atom^{-1})$] \approx -27.0$, the same value as that seen in the high redshift DLA population.

Subject headings: quasars:absorption lines—quasars:individual (HS 1543+5921) —galaxies:individual(SBS 1543+593)—galaxies:abundances

1. Introduction

Since the launch of the *Hubble Space Telescope* (HST) it has been hoped that a comparison could be made between galactic elemental abundances deduced, respectively, from emission line measurements made

[1]Based on observations with the NASA/ESA Hubble Space Telescope, obtained at the Space Telescope Science Institute, which is operated by the Association of Universities for Research in Astronomy, Inc., under NASA contract NAS5-26555.

of H II regions within some designated nearby galaxy, and ultraviolet (UV) absorption line data recorded in the spectra of a UV-bright source whose sight line passed through the same galaxy. Both measurements would yield the composition of the present-day interstellar medium (ISM) of such a galaxy, either in H II regions ionized by OB stars, or in neutral, diffuse, interstellar clouds which happen to lie in front of the background source. The initial expectation has been that the two techniques should give the same answer when applied to the same location within a particular galaxy. Indeed, for the solar neighborhood the agreement has now been verified empirically to a satisfactory degree of precision (see the discussion of this point by Esteban et al. 2004). Why, then, should we be concerned that this may not be the case in other galaxies?

One reason arises from the puzzling result that the metallicity of damped Lyα systems (DLAs) — the class of QSO absorbers with the highest column densities of neutral gas — is consistently below solar at essentially all redshifts, from $z = 0.1$ to $z > 4$ (Kulkarni et al. 2005; Prochaska et al. 2003; Pettini et al. 1999). If DLAs were representative of the galaxy population as a whole (e.g., Wolfe 1990), their element abundances should grow with time to the near-solar levels typical of today's galaxies (Fukugita & Peebles 2004). Radial abundance gradients have been appealed to as a possible explanation for the lower than solar values (Christensen et al. 2005; Chen et al. 2005; Ellison et al. 2005). Quantitatively, however, the magnitude of such gradients in nearby spirals has recently been questioned (Bresolin et al. 2004), and remains unknown at high redshifts.

A different aspect of the same 'problem' is the possibility that the H II regions of star-forming dwarf galaxies may be self-enriched in the nucleosynthetic products—chiefly oxygen—of the most massive, and short-lived, stars formed during a bout of star formation. This proposal, originally put forward by Kunth & Sargent (1986), has recently been reconsidered in the light of *Far Ultraviolet Spectroscopic Explorer* (FUSE) observations of a number of low metallicity dwarf galaxies, summarized by Cannon et al. (2005). The FUSE data seem to show that the abundances of both oxygen and nitrogen in the absorbing H I gas are systematically lower, by up to one order of magnitude, than those deduced from nebular emission lines in H II regions. Since nitrogen, a product of intermediate mass stars, is released into the ISM several hundred Myr after oxygen, such an offset may indicate the existence of an extended, lower-metallicity halo surrounding the inner star-forming regions of dwarf galaxies, rather than being evidence of self-pollution by individual H II regions.

The seemingly straightforward consistency check of measuring abundances in the spectrum of a QSO lying behind a galaxy with good emission-line metallicity diagnostics has proved deceptively difficult to carry out, since the number of suitable QSO-galaxy alignments is small: the foreground galaxy should – ideally – be at low redshift so that abundances in individual H II regions can be measured from the ground; and the background source must be bright enough in the UV to be observed at high resolution with HST, since the important diagnostic lines lie in that wavelength range. Although good QSO-galaxy alignments exist, most of the UV sources lie 1 – 2 magnitudes below the limit reachable with HST to make this technique routine.

An alternative method has been to use previously identified intermediate redshift QSO absorption systems and to measure the metallicity of the putative absorbing galaxy. In this case, light is collected across

the entire galaxy, rather than from individual H II regions, which are unresolved at such redshifts. Chen et al. (2005) conducted such a test in a few galaxies believed to be the hosts of low-redshift DLAs. Again, although there are suggestions of an offset, its origin is open to different interpretations, partly because the element measured in absorption is iron, which exhibits a highly variable degree of dust depletion in the interstellar medium (as well as having a different nucleosynthetic origin from oxygen).

The metallicity of a galaxy is, of course, closely related to the formation and evolution of its stellar population and the consequent enrichment of the interstellar medium within the galaxy. A recently developed line of inquiry into the star formation process and the regulation of the interstellar gas in DLAs has been through measurements of C II* absorption lines. The ground state of C II is split into two fine-structure levels, and the transition from one of these [the $(2p)\ ^2P_{3/2}$ level] to the first excited (^2D) state produces a C II* absorption line at 1335.7 Å. The population of the fine structure levels is determined by collisions of the C II ion with electrons and neutral hydrogen atoms, and the line can be used to measure important diagnostics. Wolfe et al. (2003b) used C II* observed in 30 high-z DLAs to infer a star formation rate (SFR) of $6 \times 10^{-3}\ M_\odot\ \mathrm{yr}^{-1}\ \mathrm{kpc}^{-2}$ for C II* arising predominantly in a cold neutral medium (Wolfe et al. 2003a, 2004). They were also able to measure a cooling rate of $\simeq 10^{-27.0}$ ergs s^{-1} H atom^{-1}, a value one dex smaller than that found by Lehner et al. (2004) for gas cooling in the Milky Way.

In this paper we present a direct comparison between emission- and absorption-based abundance determinations in a nearby galaxy and report that, unlike the previous studies reviewed above, we do find excellent agreement between the two sets of metallicity measurements.

In a previous paper (Bowen et al. 2001b) we found that the dwarf galaxy SBS 1543+593 (at a heliocentric systemic velocity of 2868 km s^{-1}— see Bowen et al. 2001a) produces a DLA in the spectrum of the background QSO HS 1543+5921 ($z_{\rm em} = 0.807$; Reimers & Hagen 1998). The QSO sight line intersects the inner regions of the galaxy, at only 2.4 arcsec, or $\simeq 0.5 h_{70}^{-1}$ kpc, from its visual center[1]. Using low-resolution spectra from HST, we found that the galaxy produced a DLA with $N(\mathrm{H\ I}) = 10^{20.35}\ \mathrm{cm}^{-2}$. From their analysis of the emission line spectrum of the brightest H II region located in a faint spiral arm 3.3 kpc from the center of the galaxy, Schulte-Ladbeck et al. (2004) concluded that the abundances of oxygen and nitrogen are approximately 1/3 and 1/10 solar respectively, consistent with the low luminosity ($M_B = -16.8$) of SBS 1543+593. In a subsequent paper, Schulte-Ladbeck et al. (2005) determined the sulfur abundance of the same emission line region to be $\simeq 0.5 \pm 0.4$ times the solar value. They also used the absorption line data presented in this paper to compare the metallicity of the neutral gas with that from the H II region, and determined that emission and absorption line measurements yield similar abundances.

In this paper, we present a detailed analysis of our data, taken with the *Space Telescope Imaging Spectrograph* (STIS) aboard HST. We refine our initial estimate of N(H I), determined originally from lower resolution STIS data, and calculate the elemental abundance of sulfur and a lower limit for the abundance of nickel. We also investigate possible ranges for the abundances of oxygen, nitrogen and silicon, and highlight

[1] $h = H_0/70$, where H_0 is the Hubble constant, and $q_0 = -0.55$ is assumed throughout this paper. No corrections are made for the velocity of the Milky Way relative to the Cosmic Microwave Background.

the uncertainty in the results which arise from using the available STIS data. Of particular concern is the question of how much of the observed S II absorption might actually arise in ionized gas, and not just from the neutral component measured from the Lyα line. We perform conventional photo-ionization modeling to show that most of the S II comes from the same neutral component traced by the H I; however, we also develop a new method to calculate an ionization correction based on a plausible measure of the star formation rate along the line of sight, and the partial measurement of the C II* λ1335.7 line found to arise in SBS 1543+593. This method again predicts that most of the S II arises in the H I absorbing medium. We conclude by comparing our abundances with those measured in the H II regions of SBS 1543+593, as well as those found in DLAs. We comment briefly on the fact that the cooling rate of the cool neutral medium in SBS 1543+593 may well be similar to that of the DLAs.

2. Data Acquisition and Analysis

2.1. Observations

An ideal observation of HS 1543+5921 would use an echelle mode of STIS to record many interstellar absorption lines simultaneously. Unfortunately, the QSO is too faint to be observed in a reasonable allocation of HST time. However, HS 1543+5921 is located in the continuous viewing zone (CVZ) for HST, which made it possible to observe using the G140M medium-resolution grating. We used the G140M at three wavelength settings (see Table 1) to record 55 Å-wide portions of the ultraviolet spectrum using the 52x0.1 aperture. The resolution of these observations is ~ 20 km s^{-1} (Kim Quijano 2004). To reduce the effects of fixed-pattern noise, data were taken using the dither pattern `STIS-ALONG-SLIT`, which moved the QSO along the slit in increments of 0.55 arcsec. As a result, spectra were recorded at one of three possible positions on the detector.

In choosing which atomic transitions to cover, we were guided by the low resolution (G140L) spectrum of the QSO (Bowen et al. 2001b) which showed that the O I λ1302 line and the N I $\lambda\lambda$1199, 1200.2, 1200.7

Table 1. Journal of Observations[a]

Date	Exposure Time (s)	CVZ Orbits	Central Wavelength (Å)	Absorption Lines Covered
2003 Aug 12	25 250	5	1222	Lyα; N I $\lambda\lambda$1199, 1200.2, 1200.7; Si III λ1206
2003 Aug 10	39 550	8	1272	S II $\lambda\lambda$1259, 1253, 1250; Si II λ1260
2004 Jan 29	14 400	3	1272	S II $\lambda\lambda$1259, 1253, 1250; Si II λ1260
2004 Jan 27	49 500	10	1321	O I λ1302; Ni II λ1317; C II λ1334; C II$*$ λ1335; Si II λ1304

[a]All the observations were conducted under GO program 9784. All data were taken with the 52x0.1 aperture.

triplet are likely to be saturated (as is usually the case in DLAs). Furthermore, at z_{DLA} = 0.0096, the N I lines fall on the wing of the Milky Way damped Lyα absorption line, where the flux is reduced to only $\sim 1 \times 10^{-15}$ ergs cm^{-2} s^{-1} Å^{-1}, too low to enable us to record these features with adequate S/N.

For these reasons, our first tilt setting of the G140M grating was chosen to record the S II $\lambda\lambda$1259, 1253, 1250 triplet which we expected to be weak and unsaturated, yet detectable in a reasonable exposure time. Sulfur is a good proxy for oxygen; like oxygen (and nitrogen) it is largely undepleted by dust in the Galactic ISM and, being an α-capture element, its abundance tracks that of oxygen in Galactic metal-poor stars (Nissen et al. 2004). Ionization corrections are expected to be small for both O I and S II when N(H I) is large.

Our second tilt was set to record a relatively short exposure with the grating centered at 1222 Å to cover the Lyα absorption line from SBS 1543+593, and thereby measure a precise H I column density. The N I triplet absorption was observed at the same time, and while the low S/N was not expected to be a major concern for the damped Lyα line (which covers many resolution elements), we knew that the short exposure time would make our observations of the N I triplet of little use.

Finally, we included observations centered at 1321 Å to cover the Ni II λ1317 absorption line. This line is of interest because nickel is a highly depleted element in local interstellar gas. Thus, the Ni II/S II ratio, when compared to its solar value, should give an indication of the degree to which refractory elements are depleted onto dust in the ISM of SBS 1543+593. This grating tilt also included O I λ1302, C II λ1334, and C II* λ1335 absorption from the dwarf galaxy. These lines were expected to be of limited use, but as we show below, we were actually able to use them to impose some constraints on physical conditions in the absorbing gas.

2.2. Data extraction

The pipeline reduction of the spectra centered at 1222 Å proved inadequate for the smooth removal of the geocoronal Lyα emission line, and provided an incorrect estimate of the background—significant counts were observed at the bottom of the Lyα profiles, where the flux was expected to be zero. Since these problems arise from poor extraction of one-dimensional (1D) spectra from the two-dimensional (2D) frames, we embarked on an optimal extraction using the prescription given by Horne (1986). We extracted data from the pipeline science-flatfielded (.flt) 2D files, and used the wavelength arrays of the pipeline extracted (.x1d file) spectra for calibration. Error arrays were also generated, using the prescription detailed by Horne (1986). Sensitivity functions were created by dividing the counts by the flux in the pipeline-calibrated spectra. When compared, the final optimally extracted spectra appeared very similar to the pipeline data, except that our extraction provided: cleaner subtraction of the geocoronal Lyα line; the removal of the correct amount of background; and the elimination of more hot pixels. Final co-addition required re-sampling individual spectra to a common wavelength scale, then adding each spectrum weighted by the inverse of its variance.

3. Ion Column Densities and Element Abundances

Below, we discuss in detail all of the absorption lines of interest which are relevant to our analysis of the metallicity of the interstellar gas in SBS 1543+593. In deriving ion column densities from the analysis of the absorption lines, we adopt wavelengths and f-values for the transitions from the extensive compilation by Morton (2003). For the Ni II λ1317 oscillator strength, we use a new value determined by Jenkins & Tripp (2005). When element abundances are compared with their solar counterparts, we use the recent reassessment of the solar abundance scale by Lodders (2003).

3.1. H I

As can be seen from Figure 1, we detect two wide damped Lyα absorption lines, from the Milky Way disk at $z \simeq 0$ and from SBS 1543+393 at $z \simeq 0.009$, respectively, as expected from the lower resolution spectrum presented in Bowen et al. (2001b). Unfortunately, the wavelength range covered by the G140M grating centered at 1222 Å is not wide enough to encompass the amount of QSO continuum on either side of the two Lyα features which is needed to normalize the data. We therefore used the spectra taken with the grating centered at 1272 Å, which overlap the shorter wavelength data by $\simeq$ 4 Å, to better define the continuum. The two sets of observations used were obtained within a few days of each other (see Table 1), so we would expect no variations in the level of the QSO flux between the two spectra. The adopted continuum, shown in Figure 1 along with the 1σ error to the fit, was derived using the method described in Sembach & Savage (1992) which uses a least-squares fit of Legendre polynomials to intensities in regions selected either side of a particular absorption line. This results in three normalized spectra: the spectrum normalized by the best fit, and two other spectra normalized by the 'upper' and 'lower' 1σ envelopes.

To measure the H I column density, N(H I), we fitted theoretical Voigt profiles to the data. Details of the fitting procedures can be found in Bowen et al. (1995). Briefly, theoretical profiles are generated from initial guesses of the column density, N, velocity, v, and Doppler parameter, b, of the absorber. After convolution with the instrumental Line Spread Function (LSF), the resulting line profile is compared with the observed one; a χ^2 minimization approach is then used to deduce the best-fitting values of N, b, and v. The LSF used was that appropriate for the G140M grating at 1200 Å,[2] although the Lyα lines in the spectrum of HS 1543+5921 are so wide that the shape of the LSF has no influence on the derivation of N(H I).

We fitted blended profiles simultaneously to both Lyα absorption lines from SBS 1543+593 and from the Milky Way disk. Wavelengths covering other narrow absorption lines were masked out. There are two sources of error in the resulting values of N and v [The shape of the Lyα profile is independent of b for such a large N(H I)]. The first arises from errors in the continuum fitting. These can be estimated by refitting the spectrum as normalized by the 1σ upper and lower continua. The second source of error in the profile fits arises from Poisson noise. To estimate the contribution from this source, we performed a Monte-Carlo

[2]see http://www.stsci.edu/hst/stis/performance/spectral_resolution/

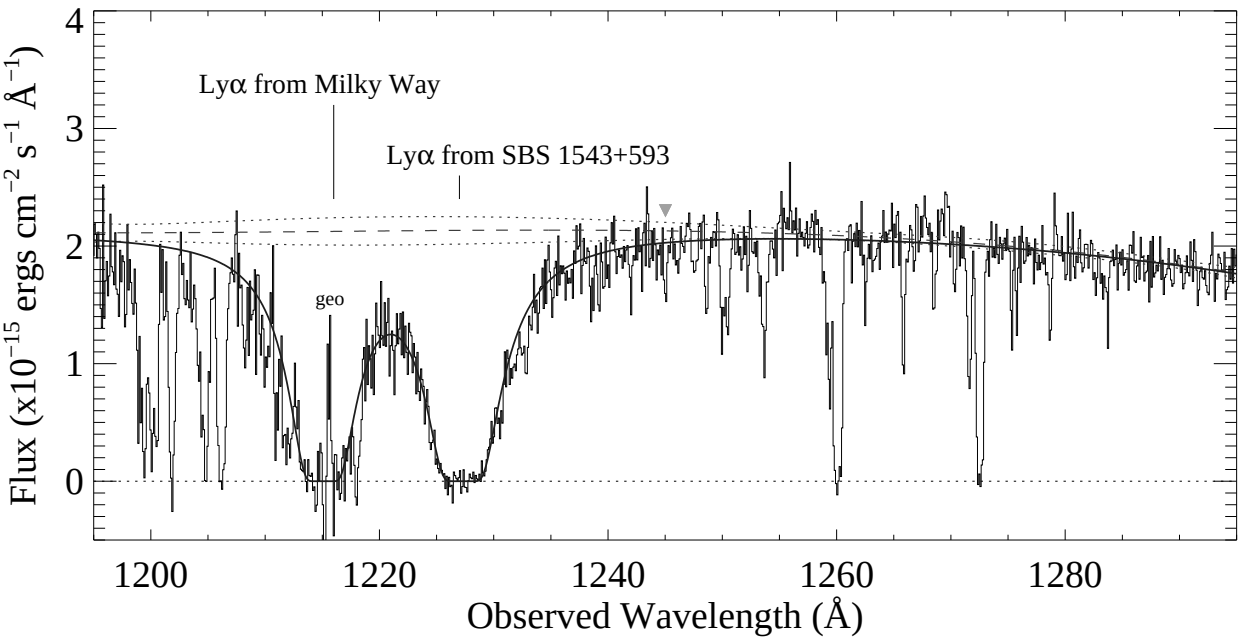

Fig. 1.— Merged STIS spectra of HS 1543+5921 taken Aug-2003, with the G140M grating centered at 1222 Å (25.25 ksec total exposure) and 1272 Å (39.55 ksec; the gray triangle denotes the wavelength at which the data were joined. Data redward of this were obtained at the same epoch as the blue data but represent spectra from only 8 of the 11 orbits which were eventually used. Hence the S/N of the data redward of the triangle is less than that of the final combined spectrum used for analysis of the absorption lines.) The damped H I Lyα lines due to absorption from both the Milky Way and SBS 1543+489 are indicated. Theoretical Voigt profile fits to these features are overplotted, along with the continuum adopted (dashed line) and its $\pm 1\sigma$ deviations (dotted). For the purposes of this figure, the data have been rebinned two pixels into one. The label "geo" indicates residual geocoronal Lyα emission.

approach, as outlined in Bowen et al. (1995). We used the theoretical best-fit profile as a starting point and added to this synthetic spectrum the same amount of noise present in the data. The lines were then refitted, resulting in a new set of values of N, v, and b. We repeated this process 500 times, then examined the distributions of N, b and v. These distributions were well approximated by Gaussians, and we used the limits which encompass 68% of the values as estimates of our random error in these parameters.

The result of this analysis yielded $\log N(\mathrm{H\ I}) = 20.42 \pm 0.04 \pm 0.01$ at a velocity of 2882 ± 16 km s^{-1}, where the first error denotes the uncertainty in column density arising from continuum placement, and the second error represents that arising purely from Poisson noise. The error in v from continuum placement is negligible. These results are summarized in Table 2. By adding these errors in quadrature, we adopt an H I column density of $\log N(\mathrm{H\ I}) = 20.42 \pm 0.04$. The central velocity of the H I absorption can be compared to the value of 2868 km s^{-1} derived from 21 cm emission measurements (Bowen et al. 2001a). The difference of 14 km s^{-1} corresponds to approximately one detector pixel for G140M data and is consistent with the known errors of 0.5−1.0 pixels in the absolute wavelength scale of STIS MAMA observations (Kim Quijano 2004). However, the velocity of the *metal* absorption lines discussed below, 2881 km s^{-1}, is very close to

the Lyα absorption velocity; since the metal lines were recorded at different grating tilts and, in some cases, at different epochs, the consistency in their velocities suggests that a value close to 2881 km s^{-1} does indeed represent the absorption system velocity, offset some 13 km s^{-1} from the systemic velocity of the galaxy, as measured from 21 cm observations.

3.2. S II

The S II $\lambda\lambda 1259.52, 1253.81, 1250.58$ triplet is clearly detected at the absorption redshift of SBS 1543+593 (see Figure 2). We define the velocity of the metal absorption line system to be 2881 km s^{-1} based on the strength, S/N, and symmetry of the Si II λ1260 line (see §3.5). With v fixed to this value, Voigt profile fits to the S II triplet give N(S II) = $1.55 \pm 0.14 \pm 0.08 \times 10^{15}$ cm^{-2} and b = $38.5 \pm 2.9 \pm 2.7$ km s^{-1}. The latter measurement suggests that the S II lines are resolved. As can be seen from the breakdown in the errors, the continuum around the S II lines shows variations on scales of a few Å, and the resulting continuum errors are significant. Again, by adding the errors in quadrature, we arrive at the adopted column density of $\log N$(S II) = 15.19 ± 0.04.

We can compare this value of N(S II) with that derived using the Apparent Optical Depth (AOD) method (Savage & Sembach 1991; Jenkins 1996), which measures column density as a function of velocity, $N_a(v)$. The AOD method provides an important check on the results from the profile fitting analysis: if the lines of the S II triplet contain any unresolved, saturated components, the $N_a(v)$ profiles of the stronger transitions (higher f-values) would appear depressed compared to the weaker ones. A comparison of $N_a(v)$ for each of the three members of the S II triplet shows no obvious evidence for saturation, to within the errors for each line. The column density for each line, integrated over a conservative velocity range of $-200 < v < 200$ km s^{-1}, is given in the last column of Table 2. If we again add the separate errors in quadrature, and weight each line by its error, we calculate a weighted average of $\log N_a$(S II) = 15.19 ± 0.06, which is identical to the value derived from profile fitting.

Dividing by the neutral hydrogen column density, we find $\log N$(S II)/N(H I) = -5.22 ± 0.06. Adopting the solar abundance $\log(\mathrm{S/H})_\odot = -4.81 \pm 0.04$ and taking (S/H) = N(S II)/N(H I), we reach the conclusion that

$$[\mathrm{S/H}] = -0.41 \pm 0.06$$

where we have used the usual logarithmic notation[3]. Hence the sulfur abundance in SBS 1543+593 is 0.39 ± 0.05 times the solar value. We discuss the validity of the assumption that (S/H) = N(S II)/N(H I) in detail in §4.

[3] [X/Y] = log(X/Y) – log(X/Y)$_\odot$

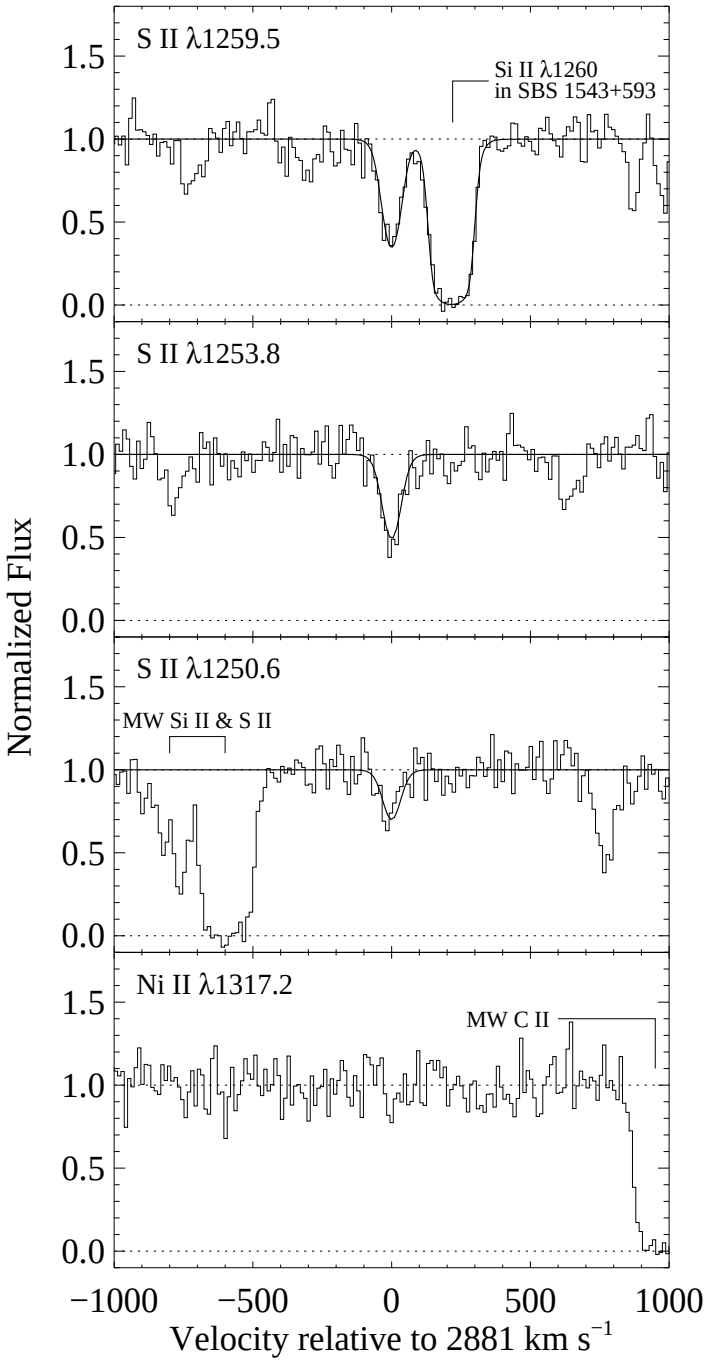

Fig. 2.— The top three panels show the S II lines arising in SBS 1543+593. Theoretical Voigt profiles which best fit the data are overplotted, generated using values of $\log N(\mathrm{S\ II}) = 15.19$, $b = 38.5$ km s^{-1}, and $v = 2881$ km s^{-1}. (The S II λ1259 line is blended with Si II λ1260, which is fit with a line profile using the values given in Table 2.) The bottom panel shows the expected position of Ni II absorption from the galaxy. Although a weak feature may appear to be present, it is not statistically significant.

Table 2. Measurements of absorption lines arising from SBS 1543+593

Ion	λ (Å)	f-value	Profile fits[a] $v_\odot$ (km s^{-1})	b (km s^{-1})	log$N$ (log [cm^{-2}])	logN_a[a,b] (log [cm^{-2}])
H I	1215.670	0.4162	2882±16	···	20.42±0.04±0.01	···
S II	1259.518	0.0166				15.18±0.05±0.04
	1253.805	0.0109	2881±2	38.5±3.0±2.6	15.19±0.04±0.02	15.25±0.10±0.05
	1250.578	0.0054				15.18±0.26±0.11
Ni II	1317.217	0.0571	···	···	···	$<$ 13.83[c]
O I	1302.168	0.0486	···	···	$\geq$ 16.2[d]	$>$ 15.3[e]
Si II	1260.422	1.1800	···	$\leq$ 41	$\geq$ 15.1	$>$ 15.0[e]
	1304.370	0.0863				
Si III	1206.500	1.6300	···	···	$\geq$ 14.5[d]	$>$ 13.9[e]
C I	1277.245	0.0853	···	···	···	$<$ 13.56[c]
C II*	1335.708	0.1283	···	···	14.28±0.15	···
Si II*	1264.738	1.0500	···	···	···	$\leq$ 12.55[c]

[a]Where more than one error is given, the first error indicates the uncertainty arising from continuum errors, while the second indicates that from Poisson noise.

[b]Column densities derived from the AOD method, with $N_a(v)$ integrated over $-200 < v < 200$ km s^{-1}, where v = 2881 km s^{-1}.

[c]2σ AOD column density limits, derived from continuum and noise errors calculated over a velocity interval $-80 < v < 80$ km s^{-1}, where v = 2881 km s^{-1}.

[d]This lower limit comes from a fit to the line assuming b and v equal that of the S II line given in row 3.

[e]Pixels with optical depths $\tau > 3$ are set to $\tau = 3$ when calculating this limit.

3.3. Ni II

The wavelength at which Ni II λ1317.217 absorption is expected from SBS 1543+593 (1329.85 Å) lies in a relatively clean part of the spectrum. A weak feature may be present at the correct wavelength (see Figure 2), but the line is not statistically significant. We measured the AOD column density over a velocity interval of $-80 < v < 80$ km s^{-1} either side of the velocity at which the Ni II line is expected. This velocity range corresponds approximately to the total width of the S II λ1250.58 line (see Figure 2). Since this S II transition is usually much stronger than the Ni II λ1317 line, it is highly unlikely that a Ni II line would be wider than the observed S II line. The measured column density over this velocity interval is 3.23×10^{13} cm^{-2}. In comparison, the continuum error is 2.13×10^{13} cm^{-2}, while the error from the noise is 2.64×10^{13} cm^{-2}. Adding these errors in quadrature yields a total 2σ error of 6.75×10^{13} cm^{-2}, or $\log N(\mathrm{Ni\ II}) < 13.83$. Since the measured column density is roughly half this value, we confirm that Ni II is undetected at the 2σ level.

Dividing by N(H I) as before, we find $\log N(\mathrm{Ni\ II})/N(\mathrm{H\ I}) < -6.59$. Subtracting the solar abundance $\log(\mathrm{Ni/H})_\odot = -5.78 \pm 0.03$, and taking (Ni/H) = N(Ni II)/N(H I), we obtain

$$[\mathrm{Ni/H}] < -0.81$$

We conclude that, in the interstellar gas of SBS 1543+593, nickel is less abundant than sulfur by at least a factor of 2.5.

3.4. O I & N I

The analysis of the O I λ1302.2 line required some additional data processing. The spectrum showed evidence of defective pixels or another source of non-random noise in the core of the absorption line. Since we shifted the target along the long axis of the slit between exposures, we were able to investigate this problem by comparing individual spectra lying at different positions on the detector. Of the eight sub-exposures of HS 1543+5921 acquired, spectra were recorded at one of three possible locations. We found clear evidence for two hot pixels at wavelengths close to the core of the O I line in two sub-exposures *which were recorded at the same position on the detector* (Archive root names o8mr05030 and o8mr06030). A third sub-exposure (o8mr05050) also appeared to be unusually noisy (at all wavelengths) compared to others. Excluding these three sub-exposures from the total improved the S/N ratio in the region of the O I λ1302 line.

As expected, the O I λ1302 line is strongly saturated (see Figure 3). We used both the AOD method and Voigt profile fitting to set lower limits to the corresponding column density of O I. In the first case, we set all pixels within the line with optical depth $\tau > 3$ to $\tau = 3$, the limit beyond which we can no longer measure the optical depth reliably. Integrating over the same velocity interval as the S II lines, $-200 < v < 200$ km s^{-1}, we obtain $\log N_a(\mathrm{O\ I}) > 15.3$.

The second method involves finding the lowest column density which will produce an acceptable fit

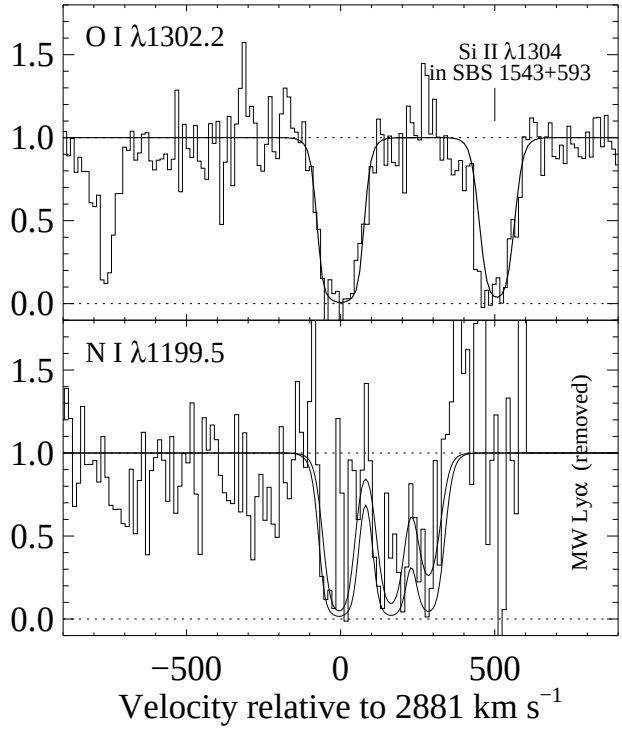

Fig. 3.— Absorption lines arising from SBS 1543+593 for which, at best, only limits to ion column densities can be reliably derived. **Top:** The O I λ1302 line profile plotted over the data represents a best fit for a component with b(O I) = b(S II) = 38.5 km s^{-1}. **Bottom:** With the damped Lyα profile from the Milky Way removed, the N I triplet has too low a S/N for a reliable column density to be measured. We overplot two sets of profiles, each with the same b value as S II, corresponding to the range of column densities of N I implied by the H II region abundance determinations of Schulte-Ladbeck et al. (2004): log$N$(N I) = 14.9 and 15.4.

to the observed line profile. Keeping v fixed to that of S II, and allowing b and N to vary, we find that b = 49.7 km s^{-1} and log$N$(O I) = 15.59. However, there exists one line of reasoning which suggests N(O I) is larger than this. We expect O I to follow H I closely, since charge exchange locks the ionization of oxygen to that of hydrogen (Field & Steigman 1971). On the other hand, while we expect most of the S II to also arise in the H I material, it is possible that some of the S II might arise in H II gas. The velocities of these ionized components may or may not be different from those of O I components, but however they are arranged in velocity, we would expect the O I line to be as narrow, or narrower, than the S II line, i.e. b(O I) $\leq$ b(S II). (For this to be true, [S/O] must be $\sim$ 0 in the absorbing regions, which is a reasonable assumption considering that both species are α-capture elements.) This condition is *not* met when N and b are allowed to vary for a fit to the O I line: as stated above, b(O I) = 49.7 km s^{-1}, whereas we measured b(S II) = 38.5 km s^{-1} in §3.2. We therefore consider that a better limit is obtained by fixing b(O I) $\leq$ b(S II) = 38.5 $\pm$ 4.0 km s^{-1}. With this constraint, we find that log$N$(O I) $\geq$ 16.2. This fit is shown in Figure 3. If b is uncertain by $\pm$4 km s^{-1}, so that b(O I) = [42.5,34.5] km s^{-1}, then log$N$(O I) = [15.9,16.6]. This value of N(O I) remains a lower limit since b(O I) could in principle be narrower than b(S II).

Adopting $\log N(\mathrm{O\ I}) \geq 16.2$ as the lower limit, we derive $\log N(\mathrm{O\ I})/N(\mathrm{H\ I}) \geq -4.2$. Since (O/H)= N(O I)/N(H I), and $\log(\mathrm{O/H})_{\odot} = -3.31 \pm 0.05$, we find that the lower limit to the oxygen abundance in SBS 1543+593 is

$$[\mathrm{O/H}] > -0.9$$

Although we believe the criterion $b(\mathrm{O\ I}) \leq b(\mathrm{S\ II})$ is a reasonable assumption, we should note that such a posit is not completely robust. Since the O I λ1302 transition is so strong, it is always possible that weak O I high-velocity components could be present which have no counterparts in the S II lines, simply because the S II f-values are not high enough to produce any absorption. These O I components could blend with the main profile in such as way that the measured b value becomes greater than the b value of S II. Nevertheless, as can be seen in Figure 2, the O I profile is remarkably close to the theoretical line profile for a single component. For high velocity O I components to widen the observed line profile, they would have to blend symmetrically on both sides of the main profile, and decrease in strength as their velocity increased away from the main absorption complex.

Our data provide even fewer constraints on the N I abundance in SBS 1543+593. The bottom panel of Figure 3 shows the N I triplet after removal of the Milky Way damped Lyα profile. The S/N is extremely low, and although absorption is present, the lines of the triplet are ill-defined. Schulte-Ladbeck et al. (2004) measured log(O/H)= -3.8 ± 0.2 from the emission lines of the brightest H II region in the south-west outer spiral arm of the galaxy. They also determined that log(N/O) lay between −1.7 and −1.2. It follows that log (N/H) lies between −5.5 and −5.0 for gas in the H II region. We can use the value of N(H I) measured above, and predict that, if the interstellar gas along the sightline had the same metallicity as the H II region, we should measure $\log N(\mathrm{N\ I})$ between 14.9 and 15.4 [again assuming that (N/H) = N(N I)/N(H I)]. Model N I lines, given these column densities and the same b value found for the S II triplet, are shown plotted over the data in Figure 3. We can say that the data are roughly consistent with these column densities, but we cannot distinguish between the upper and lower values of $\log N(\mathrm{N\ I})$.

3.5. Si II & Si III

A lower limit to the Si II column density can be derived in a similar way to that described for O I in §3.4. Both Si II λ1260.4 and 1304.4 lines are detected in the ISM of SBS 1543+593: the 1304.4 Å line has the smaller f-value and is the least saturated of the two, so should give a more reliable column density; the 1260.4 Å line is more saturated, but its inclusion in the process of fitting a theoretical line profile ensures that the b value does not become too wide. With b and N allowed to vary, we find $\log N(\mathrm{Si\ II}) \geq 15.1$ and $b(\mathrm{Si\ II}) \leq 41$ km s^{-1}.

We also note the detection of Si III in absorption from SBS 1543+593 which appears in the red wing of the damped Lyα absorption profile from the Milky Way. The line is recorded at low S/N, but is of some use in providing information on the ionization state of the gas, discussed in §4.1 below. Using the AOD method to set a conservative lower limit, we arrive at $\log N_a(\mathrm{Si\ III}) > 13.9$, after again setting all points with optical depth $\tau > 3$ to be $\tau = 3$. A Voigt profile fit to the line keeping v fixed at 2881 km s^{-1} and letting b and N

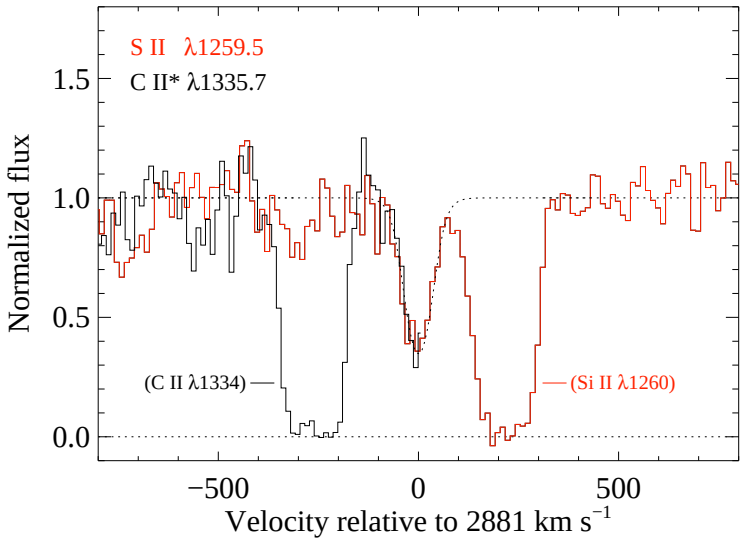

Fig. 4.— The C II* λ1335.7 absorption line (black,solid) overplotted on the S II λ1259.5 line (red,solid), both of which arise in the ISM of SBS 1543+593. Although the C II* line falls right at the edge of our spectrum, the portion which remains suggests that the line is of similar strength and shape as the S II line. (Other interstellar lines from the ISM of SBS1543+593 are labelled.) A theoretical C II* line profile with the same b and v derived for the S II triplet, generated with $\log N(\mathrm{C\ II^*}) = 14.28$ (see Table 2) is shown as a black dotted line.

vary produces the same Si III column density. We can also set $b(\mathrm{Si\ III}) \leq b(\mathrm{S\ II})$ as we did for O I; we then find $\log N(\mathrm{Si\ III}) \geq 14.5$. Although the data are of too low a quality to provide a rigorous estimate of the Si III column density, the similarity of these results suggests that our derived lower limit to N(Si III) may be robust.

3.6. C I

As we discuss in §5, even though no C I λ1277 is detected from SBS 1543+593, a limit on the C I column density is of interest for deriving limits on the electron density within the H I absorbing gas. The 2σ column density limit, again measured over the velocity interval of $-80 < v < 80$ km s^{-1}, and combining noise and continuum errors in quadrature, is 3.64×10^{13} cm^{-2}, or $\log N(\mathrm{C\ I}) < 13.56$; the measured column density in the same interval is only 1.58×10^{13} cm^{-2}.

3.7. C II*

The C II* λ1335 line arising from SBS 1543+593 lies at the very edge of the spectrum taken with the G140M grating centered at 1321 Å. Unfortunately, only half of the line is recorded (see Figure 4). Nevertheless, C II* is extremely valuable in providing insights on the conditions inside the gas clouds which give rise to the S II and C II absorption lines.

Figure 4 shows that the portion of the C II* absorption we observed has a strength and shape that are virtually identical to the corresponding part of the S II λ1259.5 line. If the velocity structures of the two species are the same, then so are the optical depths of each line, and we can state that N(C II*) = $(f\lambda)_{1259.5}N$(S II)/$(f\lambda)_{1335.7}$ = $10^{14.28}$, even if the two lines are somewhat saturated[4]. A Voigt profile with this column density, and v and b fixed to that of the S II lines, fits the visible line profile quite accurately, as can be seen in Fig 4. We can estimate an approximate error on N(C II*) by seeing how the fit changes as N changes, again keeping v and b fixed to the S II values. Although this is somewhat more uncertain than a fit to an entire line profile, we estimate that N(C II*) is accurate to within $\pm$0.15 dex.

4. Physical conditions in the ISM of SBS 1543+593

4.1. Ionization corrections to the neutral gas: CLOUDY modeling

In the previous sections, we assumed that ionization corrections can be neglected in the derivation of abundances. To test whether this is a reasonable assumption, we have assembled photoionization models as described in Tripp et al. (2003) using CLOUDY (v96; see Ferland et al. 1998 for a general description of the code) with the H I fixed at log N(H I) = 20.42 and [M/H] = –0.41. Since the sight line obviously passes through the disk of SBS 1543+593 and starlight is readily apparent nearby (see Figure 2 in Bowen et al. 2001b or Figure 1 in Schulte-Ladbeck et al. 2004), we have assumed that the gas is photoionized mainly by starlight in the disk of a galaxy. To approximate the ionizing flux, we have assumed that the shape of the radiation field is similar to that in the diffuse ISM in the disk of the Milky Way, and we have employed the Galactic disk radiation field recently presented by Fox et al. (2005, see the "0 kpc" curve shown in their Figure 8). Given the large number of H II regions distributed across the disk of SBS 1543+593, this seems like a suitable model. It is difficult to estimate the intensity for normalization of the ionizing flux field, but since the predicted columns are primarily dependent on the ionization parameter U ($\equiv$ ionizing photon density/total H number density = $n_\gamma/n_{\rm H}$), the main effect of changing the normalizing flux intensity is to change the corresponding $n_{\rm H}$ implied by the model; the relative column densities remain the same when n_γ and $n_{\rm H}$ are scaled up or down by the same amount.

Figure 5 compares the photoionization model column densities to observational constraints including the measured N(S II) and the 2σ upper limit on N(Ni II). We also show the Si III column obtained by fitting the Si III profile with the b–value allowed to freely vary (lower value) and with b forced to have the same value as the S II lines (upper value in Figure 5). Even the higher value for N(Si III) could significantly underestimate the true column due to saturation and an uncertain b–value.

Figure 5 shows two interesting results. First, even though there can be substantial amounts of ionized gas in a gas slab with the SBS 1543+593 H I column that is photoionized by starlight (as revealed by the Si III curve), the ionization corrections for S II and Ni II are likely to remain rather small or negligible. The

[4]For the C II* absorption, we assume that the 1335.663 and 1335.708 Å transitions are equivalent to a single transition with log $f\lambda$ = 2.234.

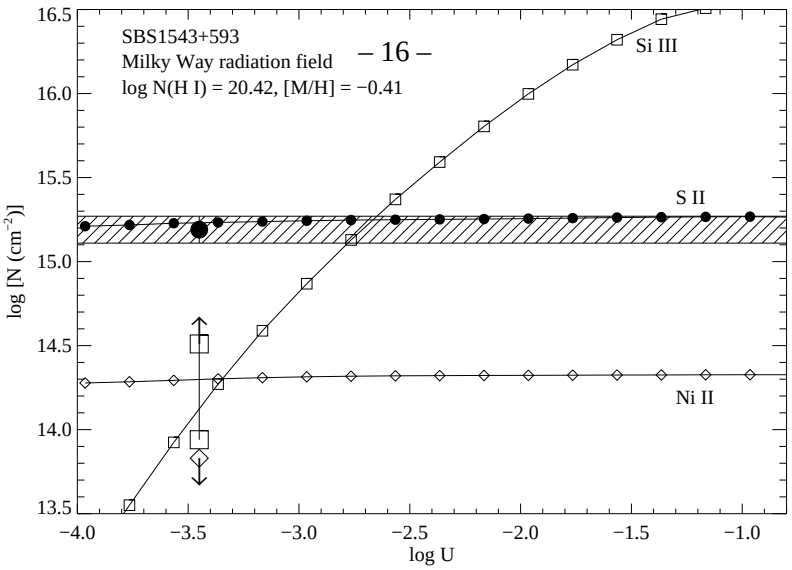

Fig. 5.— Column densities of S II (filled circles), Ni II (open diamonds), and Si III (open squares) predicted by a CLOUDY photoionization model for a gas slab with log N(H I) = 20.42, overall metallicity [M/H] = −0.41, and solar relative abundances of S, Ni, and Si. The ionizing radiation field was assumed to be similar to the radiation field estimated by Fox et al. (2005) for the diffuse ISM in the disk of the Milky Way (see the "0 kpc" curve shown in Figure 8 of Fox et al.). The model column densities are shown with small symbols and are plotted as a function of the ionization parameter U. The observed column densities are shown with larger symbols at log $U \approx -3.45$; the hatched region indicates the range of log N(S II) consistent with the observed S II column within $\pm 2\sigma$. Two values for N(Si III) are shown corresponding to different assumptions about the Si III b–value; conservatively, these should both be treated as lower limits (see text).

reason for this is that while the ion fractions f (averaged over the thickness of the gas slab) of H I, S II, and Ni II steadily decrease as U increases, over the entire range of U shown in Figure 5, f(H I) $\approx$ f(S II) $\approx$ f(Ni II), so that ionization corrections are not necessary (see eqn. 2 in Tripp et al. 2003). Indeed, the strong Si III absorption detected in the SBS 1543+593 DLA is entirely consistent with a simple photoionized gas slab, i.e., there is no need based on the current data to invoke a more complex multiphase model. The Si III arises in the ionized surface layer of the gas slab, but most of the H I, S II, and Ni II is located in the shielded interior of the slab. Second, the underabundance of Ni II is probably not an ionization effect. Over a wide range of U, we find little change in N(S II)/N(Ni II), and at all values of U that we have considered, the model predicts a significantly higher Ni II column than the 2σ upper limit.

We must note, however, that this model is not unique. It is straightforward to construct a UV radiation field which is much softer than that described above; for example, one in which the flux field is dominated by photons from an ensemble of cooler, B-type stars. In this model, hydrogen is ionized over a longer path length than for the harder flux field, and some S II arises in H II gas. Whether this UV field is applicable for SBS 1543+593 is unclear, however; since over 30 candidate H II regions are identified by Schulte-Ladbeck et al. (2004) in the the galaxy, it seems likely that some contribution to the background must come from hot O-type stars. Nevertheless, it is a concern that the sightline to the background QSO passes near the center of the galaxy, somewhat distant from the most intense areas of star formation.

A final caveat centers on the fact that it may simply be inappropriate to use a model which assumes that

a gas slab is illuminated by a background radiation field, which is the calculation that CLOUDY performs. In particular, the state of the ISM illuminated from stars and H II regions embedded in a disk may be different from that calculated by CLOUDY.

Given these uncertainties, in the following section we develop an alternative method for estimating how much S II may actually arise in ionized gas.

4.2. An Alternate Method for Determining the Ionization Correction

Our ultimate objective is to determine the fraction

$$F_{\rm H\ II}({\rm S\ II}) = \frac{N({\rm S\ II})_{\rm H\ II}}{N({\rm S\ II})_{\rm H\ I} + N({\rm S\ II})_{\rm H\ II}} \quad (1)$$

so that we can apply a multiplicative correction $\left[1 - F_{\rm H\ II}({\rm S\ II})\right]$ to our measured value of N(S II) and thereby determine the correct abundance of sulfur [S/H] in SBS 1543+593. One way to do this is to compare two different methods for deriving the expected emission measure (EM) of the ionized gas $\int n(e)^2 dl$ in the H II regions that are created by radiation from young stars during active star formation. The first procedure, discussed in §4.2.1, starts with an estimate for the star formation rate (SFR) per unit area, $\Sigma_{\rm SFR}$, based on our measured N(H I) combined with a widely applicable empirical relationship between $\Sigma_{\rm SFR}$ and gas surface density. On the assumption that little if any of the ionizing radiation from the stars is lost, we can can convert $\Sigma_{\rm SFR}$ into an expectation for the EM (§4.2.2).

The other, independent method for deriving the EM is through our observation of C II*(§3.7). However, the formulation we develop for the EM, derived in §4.2.3, involves a number of previously unknown quantities, such as the amount of multiply-ionized C in the H II regions, the apportionment of C II* between H I and H II regions, and, finally, the quantity we wish to determine, $\left[1 - F_{\rm H\ II}({\rm S\ II})\right]$. By studying the production of C II* in H I regions of our own Galaxy, we conclude in §4.2.4 that only a small fraction of the C II* in SBS 1543+593 should come from H I regions, after we compensate for differences in the star formation rates and dust grain contents in the two systems. Making use of this information, we equate the two different determinations of the EM in §4.2.5 and find that we can set a useful upper limit for the amount of S II that arises from H II regions.

4.2.1. Star Formation Rate Based on N(H I)

Unfortunately, it is difficult for us to determine the SFR near the line of sight by traditional means (e.g., stellar brightness and spectral energy distribution, the strength of Hα emission, or the far infrared brightness) because we are blinded by the flux from the quasar. Instead, we make use of a recent refinement (Kennicutt 1998a) of the Schmidt law (Schmidt 1959) that expresses an empirical relationship between the

SFR per unit area $\Sigma_{\rm SFR}$ and the surface density of (atomic plus molecular) hydrogen $\Sigma_{\rm gas}$

$$\Sigma_{\rm SFR} = 2.5 \pm 0.7 \times 10^{-4} \left(\frac{\Sigma_{\rm gas}}{1 {\rm M}_\odot \, {\rm pc}^{-2}} \right)^{1.4 \pm 0.15} {\rm M}_\odot \ {\rm yr}^{-1} \ {\rm kpc}^{-2} \tag{2}$$

that seems to apply to a broad range of galaxy types and locations within galaxies (including nuclear starbursts associated with molecular gas disks). We see no reason to believe that there could be a breakdown of this relationship caused by either prominent bars or activity related to galaxy mergers or tidal effects. Drawing from experience in our own Galaxy (Savage et al. 1977) and the Magellanic Clouds (Tumlinson et al. 2002), we expect that for our observed value of N(H I) the contribution from molecular hydrogen is unlikely to exceed a few percent of the total hydrogen. Thus, for $N({\rm H\ I}) = 10^{20.42 \pm 0.04}$ cm^{-2}, we obtain

$$\Sigma_{\rm SFR} = 7^{+9}_{-4} \times 10^{-4} \, {\rm M}_\odot \ {\rm yr}^{-1} \ {\rm kpc}^{-2} \, , \tag{3}$$

where the stated limits include the effects from the two errors shown in Eq. 2 (which are assumed to be uncorrelated), a natural rms dispersion of ± 0.3 dex of real outcomes on either side of the Schmidt law, and our uncertainty in N(H I), all combined in quadrature.

4.2.2. Anticipated Emission Measure

Assuming that there is no escape of Lyman Limit photons and that they are not absorbed by dust, we can calculate the value of the EM from $\Sigma_{\rm SFR}$. For a Salpeter (1955) IMF and solar abundances, the hydrogen-ionizing photon production rate $Q({\rm H}^0)$ in units of s^{-1} is given by

$$Q({\rm H}^0) = {\rm SFR} / 1.08 \times 10^{-53} \, {\rm M}_\odot \, {\rm yr}^{-1} \, {\rm s} \tag{4}$$

(Kennicutt 1998b). Certain factors could change the constant in Eq. 4. For instance, an IMF defined by Scalo (1986) would increase the constant by about a factor of three (Kennicutt 1998b). We acknowledge that the stars in SBS 1543+593 will have compositions below solar, but the change in ionizing fluxes should be very small (Lanz & Hubeny 2003).

If all of the ionizing photons are consumed by the ionization of H, $Q({\rm H}^0)$ per unit area must balance the product of EM and the hydrogen recombination coefficient $\alpha^{(2)}$ to all levels higher than the ground electronic state. For a temperature in the vicinity of 10^4 K (or $T_4 = T / 10^4 \, {\rm K} \approx 1$) a power-law fit to the values of $\alpha^{(2)}$ and temperature given by Spitzer (1978) yields

$$\alpha^{(2)} = 2.55 \times 10^{-13} \, T_4^{-0.833} \ {\rm cm}^3 \, {\rm s}^{-1} \, . \tag{5}$$

Thus, we find that

$$\mathrm{EM} = 1.23 \times 10^4 \, T_{4,n(e)^2}^{0.833} \, \Sigma_{\rm SFR} \ {\rm cm}^{-6} \, {\rm pc} \tag{6}$$

where, as in Eq. 3, $\Sigma_{\rm SFR}$ is expressed in the units ${\rm M}_\odot \, {\rm yr}^{-1} \, {\rm kpc}^{-2}$, and for an inhomogeneous H II region $T_{4,n(e)^2}$ is the temperature (in units of 10^4 K) weighted by the local squares of the electron densities along the line of sight, i.e., $T_{4,n(e)^2} = \int T_4 n(e)^2 dl \Big/ \int n(e)^2 dl$.

4.2.3. C II* *Contributions from H II Regions*

Collisions with electrons excite singly ionized carbon atoms to the upper fine-structure level of the ground electronic state, creating C II*. The balance between this excitation and radiative decay leads to an equilibrium equation from which one can derive the electron density

$$n(e) = \frac{g_1 A_{2,1} T^{0.5} \exp(91\mathrm{K}/T)}{8.63\times10^{-6}\Omega_{1,2}} \left(\frac{n(\mathrm{C\ II^*})}{n(\mathrm{C\ II})}\right) = 18.3\, T_4^{0.5} \exp(0.0091/T_4) \left(\frac{n(\mathrm{C\ II^*})}{n(\mathrm{C\ II})}\right)\ \mathrm{cm}^{-3}, \quad (7)$$

where the lower level's statistical weight $g_1 = 2$, the upper level's spontaneous decay rate $A_{2,1} = 2.29 \times 10^{-6}\,\mathrm{s}^{-1}$ (Nussbaumer & Storey 1981), and the collision strength $\Omega_{1,2} = 2.90$ at $T = 10^4$ K (Hayes & Nussbaumer 1984). This equation arises from a simplified form of the equilibrium equation in the limit where collisional de-excitations can be neglected, which happens when $N(\mathrm{C\ II^*})/N(\mathrm{C\ II}) \ll 1$ (which is true here) – see, e.g., Jenkins et al. 2000. Henceforth, we will drop the $\exp(0.0091/T_4)$ term since it is so close to 1.0 when $T_4 \sim 1$, which seems justified for H II regions in systems with metal contents somewhat below that of our Galaxy, such as those in M101 (Kennicutt et al. 2003). In most circumstances, optical pumping of the excited level is unimportant (Spitzer & Jenkins 1975; Sarazin et al. 1979).

An alternate expression for $n(e)$ within the H II region is given by the equation

$$n(e) = \left(\frac{\mathrm{H}}{\mathrm{C}}\right) n(\mathrm{C\ II})\, y(\mathrm{C\ II}) \quad (8)$$

where

$$y(\mathrm{C\ II}) = \frac{n(\mathrm{C\ II}) + n(\mathrm{C\ III}) + n(\mathrm{C\ IV})}{n(\mathrm{C\ II})} \quad (9)$$

In an H II region where the ionization by starlight dominates over that from an intergalactic field, the expected values of y(C II) are strongly dependent on the average temperature of the exciting stars T_*: models of ion abundances in H II regions evaluated by Stasinska (1990) indicate that the ratio of $\int n(\mathrm{C_{total}})\, n(e)\, dV \,/\, \int n(\mathrm{C\ II})\, n(e)\, dV$ varies from 1.26 for $T_* = 32,500$ K, to 8.5 for $T_* = 40,000$ K, and could reach as high as 22 for $T_* = 50,000$ K.

It is reasonable to assume that [S/C] ≈ 0 in SBS 1543+593, which permits us to arrive at an estimate for the H to C abundance ratio,

$$\left(\frac{\mathrm{H}}{\mathrm{C}}\right) = \left(\frac{\mathrm{S}}{\mathrm{C}}\right)_{\odot} \frac{N(\mathrm{H\ I})}{\left[1 - F_{\mathrm{H\ II}}(\mathrm{S\ II})\right] N(\mathrm{S\ II})} \quad (10)$$

which we consider to be a universal abundance ratio everywhere. We can now formulate a useful expression for $n(e)^2$ by taking the product of the expressions in Eqs. 7 and 8,

$$\mathrm{EM} = 5.93\times10^{-18} \left(\frac{\mathrm{H}}{\mathrm{C}}\right) \int n(\mathrm{C\ II^*})\, T_4^{0.5}\, y(\mathrm{C\ II})\, dl\ \mathrm{cm}^{-6}\mathrm{pc} \quad (11)$$

To be rigorous, we must allow for the possibility that T_4 and y(C II) could vary inside the H II region(s), and therefore we define a product

$$Y_{n(\mathrm{C\ II^*})}(\mathrm{C\ II})\, T^{0.5}_{4,n(\mathrm{C\ II^*})} = \int T_4^{0.5}\, y(\mathrm{C\ II})\, n(\mathrm{C\ II^*})\, dl \Bigg/ \int n(\mathrm{C\ II^*})\, dl \quad (12)$$

so that we can work with a more streamlined representation

$$\begin{aligned} \mathrm{EM} &= 5.93\times10^{-18}\left(\frac{\mathrm{S}}{\mathrm{C}}\right)_{\odot}\left(\frac{N(\mathrm{H\ I})}{N(\mathrm{S\ II})}\right)\ \times \\ &\left(\frac{Y_{n(\mathrm{C\ II^*})}(\mathrm{C\ II})\,T^{0.5}_{4,n(\mathrm{C\ II^*})}F_{\mathrm{H\ II}}(\mathrm{C\ II^*})}{1-F_{\mathrm{H\ II}}(\mathrm{S\ II})}\right)N(\mathrm{C\ II^*})\ \mathrm{cm^{-6}pc} \end{aligned} \tag{13}$$

after we make the substitution for (H/C) given in Eq. 10. [$F_{\mathrm{H\ II}}$(C II*) is defined in a manner identical to that for S II in Eq. 1.]

Were it not for the uncertainties in the quantities $Y_{n(\mathrm{C\ II^*})}$(C II), $T^{0.5}_{4,n(\mathrm{C\ II^*})}$, and $F_{\mathrm{H\ II}}$(C II*), we could determine $F_{\mathrm{H\ II}}$(S II) by equating the EM given in Eq. 13 with that given earlier in Eq. 6. To provide useful constraints on these unknown quantities, we must evaluate the probable contribution of C II* from H I regions.

4.2.4. An Evaluation of $F_{\mathrm{H\ II}}$(C II*)

The discussion presented in the previous subsection focused on the properties of fully ionized gas regions, as revealed by C II*, but with the retention of an unknown fractional quantity $F_{\mathrm{H\ II}}$(C II*) that expressed how much of the observed C II* actually came from such regions. We now examine the plausibility that $F_{\mathrm{H\ II}}$(C II*) could be appreciably lower than 1.0, and that a reasonable fraction $\left[1-F_{\mathrm{H\ II}}(\mathrm{C\ II^*})\right]$ of the C II* arises from H I regions, as opposed to H II regions. One way to do this in principle is to measure N(Si II*)/N(C II*) (Howk et al. 2005), since the excitation energies of the two are very different. Unfortunately, our 2σ column density limit derived at the expected position of the Si II* λ1264 line is $\log N(\mathrm{Si\ II^*}) < 12.55$. This limit is not sufficiently sensitive to discriminate between contributions from H II regions with $T_4 \sim 1$ and H I regions at much lower temperatures.

We turn now to a different, but less direct way to measure $F_{\mathrm{H\ II}}$(C II*). For the H I regions that intersect our line of sight, the average cooling rate per H atom arising from the emission of radiation at 157.7 μm caused by the radiative decay of C II* corresponds to

$$\begin{aligned} l_C &= (A_{2,1}hc/\lambda)\left[1-F_{\mathrm{H\ II}}(\mathrm{C\ II^*})\right]N(\mathrm{C\ II^*})/N(\mathrm{H\ I}) \\ &= 2.88\times10^{-20}\left[1-F_{\mathrm{H\ II}}(\mathrm{C\ II^*})\right]N(\mathrm{C\ II^*})/N(\mathrm{H\ I})\ \mathrm{erg\ s^{-1}\ H\ atom^{-1}}\,. \end{aligned} \tag{14}$$

For our measurements of N(C II*) and N(H I), we obtain $\log\left(l_C/\left[1-F_{\mathrm{H\ II}}(\mathrm{C\ II^*})\right]\right) = -25.68$. If we omit the factor $\left[1-F_{\mathrm{H\ II}}(\mathrm{C\ II^*})\right]$, this value is about the same as the rate $\log l_C = -25.70$ (+0.19, -0.35 for the 1σ dispersion of individual determinations) found by Lehner et al. (2004) for low-velocity clouds and some accompanying ionized material in the local region of our Galaxy.

For densities $n(\mathrm{H}) \gtrsim 0.1\,\mathrm{cm^{-3}}$, within the ISM of our Galaxy the heating rate from energetic photoelectrons liberated from dust grains dominates over those arising from cosmic ray and X-ray ionizations

(Wolfire et al. 1995; Weingartner & Draine 2001b). To a first order of approximation, we expect the dust grain heating to scale in proportion to both (1) the local starlight density, with special emphasis on the far-UV photons, and (2) the density of dust grains per H atom. This relationship is valid as long as there is no appreciable loss of efficiency caused by the grains acquiring a positive charge because the recombination rate with free electrons is too low – see Fig. 16 of Weingartner & Draine (2001b). A reasonably good gauge of the local far-UV starlight flux is the SFR. We can propose that the grain density should scale in proportion to the overall metal abundance, $10^{[\mathrm{M/H}]}$, although we caution that there are indications from IR emission that the character of dust in low metallicity systems, and in particular the polycyclic aromatic hydrocarbons (PAHs) which are important for heating the gas, is different from that of our Galaxy (Draine 2005; Engelbracht 2005). Thus, there may not be a simple downward scaling of the abundances of all the different kinds of dust. Nevertheless, if we overlook this possible complication and use our local region of the Milky Way (MW) as a comparison standard, we can express a proportionality

$$\frac{l_C(\mathrm{SBS\ 1543+593})}{\Sigma_{\mathrm{SFR}}(\mathrm{SBS\ 1543+593})} = 10^{[\mathrm{M/H}]} \frac{l_C(\mathrm{MW})}{\Sigma_{\mathrm{SFR}}(\mathrm{MW})}\,, \tag{15}$$

where l_C(SBS 1543+593) is defined in Eq. 14, Σ_{SFR}(SBS 1543+593) is calculated in Eqs. 6 and 13, and $10^{[\mathrm{M/H}]} = \left[1 - F_{\mathrm{H\ II}}(\mathrm{S\ II})\right] 10^{-0.41}$ (see §4.2.2). For l_C(MW) we adopt a representative value of 1.3×10^{-26}erg s^{-1} H atom^{-1}, which Lehner et al. (2004) found for low velocity clouds that have sufficient column densities to make the relative contributions of C II* from ionized regions relatively small (see their Fig. 8). An acceptable range for Σ_{SFR}(MW) in our region of the Galaxy is $(3.5-5) \times 10^{-3}\,\mathrm{M_\odot\,yr^{-1}\,kpc^{-2}}$ (Rana 1991). Using these quantities, we solve Eq. 15 to find that

$$F_{\mathrm{H\ II}}(\mathrm{C\ II^*}) = \left[1 + 0.057 T_{4,n(e)^2}^{-0.833}\, T_{4,n(\mathrm{C\ II^*})}^{0.5}\, Y_{n(\mathrm{C\ II^*})}(\mathrm{C\ II})\right]^{-1} \tag{16}$$

With some loss of rigor for nonuniform regions where both T_4 and y(C II) might vary, we can consolidate the two temperature terms with the different weightings into a single representation T_4 to obtain

$$F_{\mathrm{H\ II}}(\mathrm{C\ II^*}) = \left[1 + 0.057 T_4^{-0.333} Y_{n(\mathrm{C\ II^*})}(\mathrm{C\ II})\right]^{-1} \tag{17}$$

4.2.5. An Evaluation of $Y_{n(\mathrm{C\ II^*})}$(C II)

As we stated earlier (§4.2.3), the value of the inverse of the fraction of C atoms in the singly ionized form, $Y_{n(\mathrm{C\ II^*})}$(C II), can be slightly greater than 1 or very large, depending on the hardness of the ionizing radiation (i.e., the characteristic temperature of the exciting stars). Any constraints that we can place on the value of this parameter are critical for our being able to estimate how much of the C II* arises from H II regions (see Eq. 17 above), and this quantity is essential for our final estimate of $F_{\mathrm{H\ II}}$(S II).

If we convert the Σ_{SFR} derived from the Schmidt law (Eq. 3) to an EM using Eq. 6 and equate the result with the EM given in Eq. 13 (with the expression in Eq. 17 substituted for $F_{\mathrm{H\ II}}$(C II*)), we find that

$$\frac{Y_{n(\mathrm{C\ II^*})}(\mathrm{C\ II})}{1 + 0.057 T_4^{-0.333} Y_{n(\mathrm{C\ II^*})}(\mathrm{C\ II})} = 0.7^{+1.0}_{-0.4}\, T_4^{0.333} \left[1 - F_{\mathrm{H\ II}}(\mathrm{S\ II})\right] \tag{18}$$

(once again we have consolidated the slightly different kinds of temperature terms $T_{4,n(e)^2}$ and $T_{4,n(\mathrm{C\ II^*})}$ into a single term T_4). The uncertainty for the numerical coefficient on the right-hand side of the equation considers the uncertainty in the value of Σ_{SFR} combined with the uncertainties in the column densities of H I, S II and C II* that also appear in this result. Clearly, with $T_4 = 1$ we are unable to find an acceptable result with the preferred value of the coefficient, since we require that $Y_{n(\mathrm{C\ II^*})}(\mathrm{C\ II}) \geq 1.0$ and $F_{\mathrm{H\ II}}(\mathrm{S\ II}) \geq 0$. If this coefficient is at its (1σ) upper limit of 1.7 and $Y_{n(\mathrm{C\ II^*})}(\mathrm{C\ II}) = 1.0$, then $F_{\mathrm{H\ II}}(\mathrm{S\ II})$ could equal 0.44. However, $Y_{n(\mathrm{C\ II^*})}(\mathrm{C\ II})$ is likely to be somewhat greater than 1.0, but by an amount that is uncertain, so $F_{\mathrm{H\ II}}(\mathrm{S\ II})$ is probably lower than 0.44.

To summarize, our consideration of the Schmidt law in conjunction with our measurement of N(H I) leads to an implied SFR which, when combined with our interpretation on the origin of C II*, places an upper limit of about 44% on the relative amount of S II that could arise from H II regions.

While one might argue that in principle Σ_{SFR} could deviate above the $+1\sigma$ limit that was used to derive our upper limit for F_{HII}(S II) if the conversion rate of gas into stars were significantly higher than implied by the scaling of eq.(2), this possibility seems unlikely for a galaxy with a surface brightness as low as that of SBS 1543+593. The argument presented here, along with the one given in §4.1, means that [S/H] for the gas we detected in SBS 1543+593 is probably very close to the more naive determination based on $\log[N(\mathrm{S\ II})/N(\mathrm{H\ I})] - \log(\mathrm{S/H})_\odot = -0.41$, but it might be as low as −0.66.

5. Physical Conditions of the Gas

If we knew the column density of C II in the H II region, we could determine a representative electron density weighted by the density of C II inside it, i.e., $n(e)_{n(\mathrm{C\ II})}$. This would be done through the use of Eq. 7 (but with a replacement of local densities n with column densities N), because we know that most of the C II* arises from collisions with electrons within fully (or mostly) ionized material. Unfortunately, the information about $F_{\mathrm{H\ II}}$(S II) cannot be applied to C, because the low value of $F_{\mathrm{H\ II}}$(S II) could have arisen from the fact that y(S II) is very much greater than 1 over most parts of the region. Indeed, the models of Stasinska (1990) indicate that S reverts to multiply ionized stages more strongly than C, and this could in principle help to explain the small value of $F_{\mathrm{H\ II}}$(S II).

For the neutral material, the situation is different. Since it is virtually certain that most of the C and S is singly ionized, we can make the reasonable assumption that [C/S] = 0 and state that inside the H I region

$$N(\mathrm{C\ II}) = \left(\frac{\mathrm{C}}{\mathrm{S}}\right)_\odot \Big[1 - F_{\mathrm{H\ II}}(\mathrm{S\ II})\Big]\, N(\mathrm{S\ II}) \tag{19}$$

or

$$\log N(\mathrm{C\ II}) = 16.39 \text{ if } F_{\mathrm{H\ II}}(\mathrm{S\ II}) \approx 0 \tag{20}$$

In §3.6, we reported a limit $\log N(\mathrm{C\ I}) < 13.56$. We can use this limit together with our inferred value for $\log N$(C II) to place limits on $n(e)$ and n(H) in cool H I regions if we use the equilibrium equation for the balance of photoionizations, at a rate Γ_{C}, against recombinations with free electrons (with a rate constant

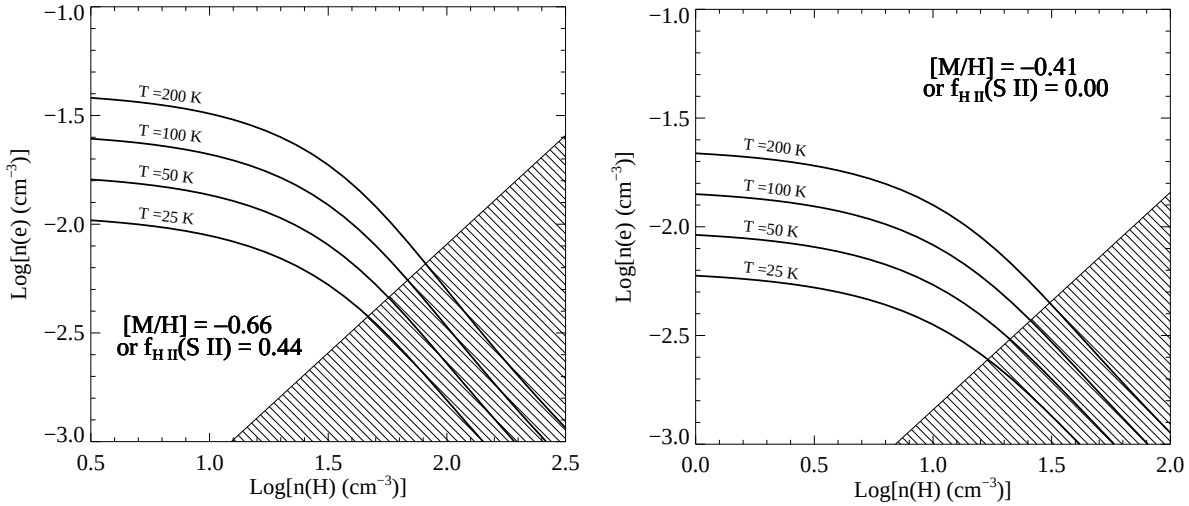

Fig. 6.— Upper bounds that satisfy Eq. 21 and our observation that $\log N(\mathrm{C\ I}) - \log N(\mathrm{C\ II}) < -2.83$, i.e., combinations of $n(e)$ and $n(\mathrm{H})$ below the curves for four representative temperatures are the only ones allowed by our observations. The left-hand panel depicts the condition that only 0.56 times our assumed column density of C II [derived from N(S II) and our assumption that [C/S] = 0] is in the H I region, while the right-hand panel shows the conditions when virtually all of the C II is in the H I region. The shaded portion in the lower right portion of each panel indicates a disallowed region where $n(e)$ is less than the product of $n(\mathrm{H})$ and the sum of the relative abundances of all elements that can be photoionized in an H I region.

α_e) and negatively charged dust grains (with a rate constant α_g),

$$[\alpha_e n(e) + 10^{[\mathrm{M/H}]}\alpha_g n(\mathrm{H})]\, n(\mathrm{C\ II}) = \Gamma_{\mathrm{C}} n(\mathrm{C\ I})\,. \tag{21}$$

Formulae for the rate constants α_e and α_g are defined by Aldrovandi & Pequignot (1973) and Weingartner & Draine (2001a), respectively. As in §4.2.4 above, when we evaluate this equilibrium we assume that the factor $10^{[\mathrm{M/H}]}$ reflects a reasonable estimate for the grain density relative to that in our Galaxy. The representative ionization rate for neutral carbon Γ_{C} should scale in proportion to Σ_{SFR} since the atoms are ionized by photons with energies greater than 11.26 eV. Thus, once again, we can scale a physical process using the Milky Way as an example,

$$\Gamma_{\mathrm{C}}(\mathrm{SBS\ 1543+593}) = \Gamma_{\mathrm{C}}(\mathrm{MW})\Sigma_{\mathrm{SFR}}(\mathrm{SBS\ 1543+593})/\Sigma_{\mathrm{SFR}}(\mathrm{MW})\,, \tag{22}$$

where $\Gamma_{\mathrm{C}}(\mathrm{MW}) = 2.24 \times 10^{-10}\mathrm{s}^{-1}$ (Jenkins & Shaya 1979).

Figure 6 shows the upper bounds for the various combinations of $n(e)$ and $n(\mathrm{H})$ that satisfy Eq. 21 and the condition that the observed $\log N(\mathrm{C\ I}) - \log N(\mathrm{C\ II}) < -2.83$, representing the case $F_{\mathrm{H\ II}}(\mathrm{C\ II}) = 0$, or the alternative that $F_{\mathrm{H\ II}}(\mathrm{C\ II})$ could be as low as our limit 0.44 for $F_{\mathrm{H\ II}}(\mathrm{S\ II})$. In effect, these two cases recognize that either a modest fraction or virtually all of the observed C II could arise from any H I region that could conceivably hold some C I.

6. Summary & Discussion

The primary goal of our STIS program was to obtain the abundance of sulfur and nickel in the interstellar medium of the galaxy SBS 1543+593, by analyzing ultraviolet absorption lines produced by the galaxy in the spectrum of the background QSO HS 1543+5921. With the good quality data obtained, and a careful analysis of the absorption lines detected (including an optimal extraction technique implemented to improve the standard pipeline extraction), we find that the abundance of sulfur is approximately two-fifths solar, [S/H] = -0.41 ± 0.06 (Table 3). This value is in good agreement with the oxygen abundance, [O/H] = -0.49 ± 0.2 deduced by Schulte-Ladbeck et al. (2004) and [S/H] $\simeq 0.3 \pm 0.3$ measured by Schulte-Ladbeck et al. (2005) from an analysis of nebular emission lines in the optical spectrum of the brightest H II region in SBS 1543+593. The most straightforward conclusion is that the two methods give a concordant picture of the degree of metal enrichment in this galaxy, at least as far as the α-capture elements—which are mostly the products of Type II supernovae—are concerned.

As is often the case, there are caveats to this conclusion. Emission and absorption line measurements do not refer to exactly the same location within the galaxy, but the two sight lines are separated by only 16.6 arcsec, or 3.3 h_{70}^{-1} kpc at the redshift of the galaxy, and low luminosity galaxies like SBS 1543+593 are found to exhibit relatively flat radial abundance gradients (de Blok et al. 1996). In deriving the sulfur abundance in the DLA, we have assumed that N(S II)/N(H I) = (S/H). This assumption would be incorrect if sulfur were depleted onto grains—a possibility which we consider far-fetched given the composition of local interstellar dust—or if some of the S II absorption arises in ionized gas which does not contribute to the damped Lyα line. If we have under-estimated the total amount of hydrogen along the sight line, then the measured abundance is only an upper limit.

Testing this last assumption has been a principle aim of this paper. Since O I tracks H I so closely in interstellar gas, an accurate measure of [O I/S II] would enable us to measure the fraction of S II arising in the observed neutral hydrogen (assuming [O/S] = 0). Unfortunately, we have only a lower limit to N(O I) from the saturated O I λ1302 line (§3.4), and can show only that [O I/S II] > -0.49. Hence we can only be certain that $>$ 32% of the observed S II line arises in neutral gas. Even the lower limit to N(O I) is subject

Table 3. Summary of Abundances in SBS 1543+593

X	$\log(X/H)_\odot$ [a]	[X/H]
S	-4.81 ± 0.04	-0.41 ± 0.06
O	-3.31 ± 0.05	> -0.9
Si	-4.46 ± 0.02	> -0.8
Ni	-5.78 ± 0.03	< -0.81

[a]Reference solar abundances taken from the collation by Lodders (2003).

to uncertainty: extra components of high velocity O I (relative to the bulk of the absorption) could arrange themselves in such as way that we adopt too narrow a Doppler parameter in calculating the lower limit, leading us to over-estimate the O I column density.

We can perhaps look to our own Galaxy to understand how the ionization stages of sulfur track neutral hydrogen. In the Milky Way, (S II/H I) ratios through the disk are exactly $[S/H]_{\odot}$ (Lehner et al. 2004) at the same H I column densities measured towards SBS 1543+593, suggesting that all the S II arises in Milky Way H I gas (assuming that most of the ISM does not have super-solar sulfur metallicities). Although conditions in the ISM of SBS 1543+593 may be different from that present in the Milky Way, it seems somewhat reassuring that at least in one high-N(H I) environment, most of the S II comes from H I regions.

Nevertheless, a more quantitative estimate of any required ionization correction would be preferable. Hence we have used the CLOUDY photoionization code to estimate how much S II arises in neutral or ionized regions. Not surprisingly, we find that the answer depends on the shape of the UV background field adopted for the calculation. If a field similar in shape to that of the Milky Way is used, then no ionization corrections are required. A much softer background though, or many embedded H II regions, could leave some of the S II arising in H II gas. Given the distribution of candidate H II regions in the galaxy identified by Schulte-Ladbeck et al. (2004), a Milky Way-like disk model seems plausible, but we acknowledge that without a real measure of the UV field near the center of the galaxy, CLOUDY models may only be a simplistic approximation of the conditions in the interstellar gas.

Given all these difficulties, we have developed a different approach to deriving an ionization correction, based on comparing two different methods for deriving the emission measure of the ionized gas (§4.2). We have used the measured N(H I) to estimate the star formation per unit area in SBS 1543+593, and from there— assuming none of the Lyman Limit photons produced by the stars escape (or are absorbed by dust) — we derive the emission measure. We have also detected C II* absorption in the ISM of the galaxy, which enables us to calculate the same emission measure. Combining these two results yields a relationship between the amount of sulfur arising in ionized gas and the amount of carbon which exists as C II. Using plausible values for the latter value leads us to believe that no more that 44% of the S II is likely to arise in ionized gas. At most, therefore, the sulfur abundance might be as low as −0.66, only 0.25 dex smaller than if we had assumed all the S II came from neutral gas.

Since we do not detect the Ni II λ1317 line, we can only deduce an upper limit to the abundance of nickel, $[Ni/H] < -0.81$ or $(Ni/H) < 1/7$ of solar. This limit implies that nickel is less abundant than sulfur by a factor of 3 or more. It seems likely that nickel is underabundant due to depletion by dust, as seen in the local ISM, where it is $\sim 10-300$ times below its solar value (e.g. Savage & Sembach 1996; Jenkins 2004). On the other hand, since nickel is an Fe-peak element synthesized mostly by Type Ia supernovae, it may be intrinsically less abundant than sulfur (and oxygen). We might expect there to be little over-abundance of alpha elements relative to iron-peak elements, since the relatively high metallicity of sulfur should imply that sufficient time has passed for Type Ia supernovae to build up the iron-peak abundances. Of course, both factors may contribute to the underabundance of nickel; in order to assess their relative importance we need to measure an undepleted Fe-peak element like zinc.

Assuming that our measured sulfur abundance is correct, it is reassuring to confirm that emission- and absorption-based abundance measurements do give consistent results, as we would expect. Of course, the case reported here refers to only one (late-type dwarf) galaxy but, as emphasized above, the test we have carried out is the 'cleanest' so far, free from the complications introduced by: (i) differences in dust depletion and nucleosynthetic origin of the elements being compared, (ii) absorption line saturation, and (iii) the geometry of composite sight lines through the absorbing medium. Our result, therefore, has implications for the interpretation of similar comparisons which have been reported recently, as we now briefly discuss.

There seems to be no need for an envelope of unprocessed, neutral gas surrounding this dwarf galaxy to contribute to the observed absorption, in contrast with the suggestion put forward by Cannon et al. (2005) in their interpretation of FUSE absorption line spectroscopy of a number of star-bursting dwarf galaxies. Possibly, this difference is related to the evolutionary status of the galaxies involved—SBS 1543+593 is more metal-rich than some, though not all, of the galaxies considered by Cannon et al. (2005) and is *not* undergoing a current burst of star formation. One could think of plausible scenarios where the existence of a metal-poor halo around galaxies may be related to both of these factors. Of course, measuring abundances in dwarf galaxies with FUSE has its own set of unique problems. For one thing, absorption lines are seen against the background light of the central starburst which is an extended, rather than point-like, source. In addition, the relatively small telescope aperture of FUSE can only record such spectra at modest signal-to-noise ratios (S/N); in these conditions the absorption lines studied tend to be strong and saturated. Had our metallicity measurements in SBS 1543+593 been based on O I λ1302 and other similarly saturated absorption lines, we may well have (erroneously) concluded that there is an order of magnitude difference between H I and H II region abundances in this galaxy too (§3.4).

As for the population of DLAs as a whole, it can be seen from Figure 7 that SBS 1543+593 is among the least metal-poor DLAs at $z < 1$ (and indeed, at any redshift). This may well be the result of the unusually low impact parameter of this QSO-galaxy pairing, as the sight line to HS 1543+5921 intersects the galaxy at $\leq$ 0.5 h_{70}^{-1} kpc from its center. In other low-z DLAs, radial metallicity gradients have been proposed to explain the finding that $[\mathrm{Fe/H}]_{\mathrm{DLA}}$ is lower than $[\mathrm{O/H}]_{\mathrm{H\ II}}$ (Chen et al. 2005). We would have found a similar result ourselves, had we based our abundance comparison on nickel (§3.3) which, like iron, can be depleted from the gas-phase of the ISM by significant, and variable, amounts. Furthermore, the systematic offsets which have recently been identified in the derivation of [O/H] from the ratios of strong nebular emission lines (Garnett et al. 2004a,b; Bresolin et al. 2004) seem to be less important when the oxygen abundance is sub-solar, as in SBS 1543+5921, than solar or super-solar, as is the case for the galaxies considered by Chen et al. (2005). These offsets would work in the sense of increasing the difference between H II and H I region abundances. Thus, in order to assess the degree to which abundance gradients are responsible for the generally low metallicities of DLAs, we need: (i) better determinations of the gradients in local galaxies and (ii) more instances like the one reported here where emission- and absorption-deduced abundances can be compared without the uncertainties associated with dust depletion and strong emission line calibrators.

The cooling rates l_c of the DLAs derived from C II* absorption lines have been investigated in detail by Wolfe et al. (2003b,a, 2004). The median value of $\log(l_c)$ in the DLA population is $\simeq -27.00$ (where l_c is in units of ergs s^{-1} H atom^{-1}). Calculating l_c for SBS 1543+593 relies on knowing the fraction of C II* in H II

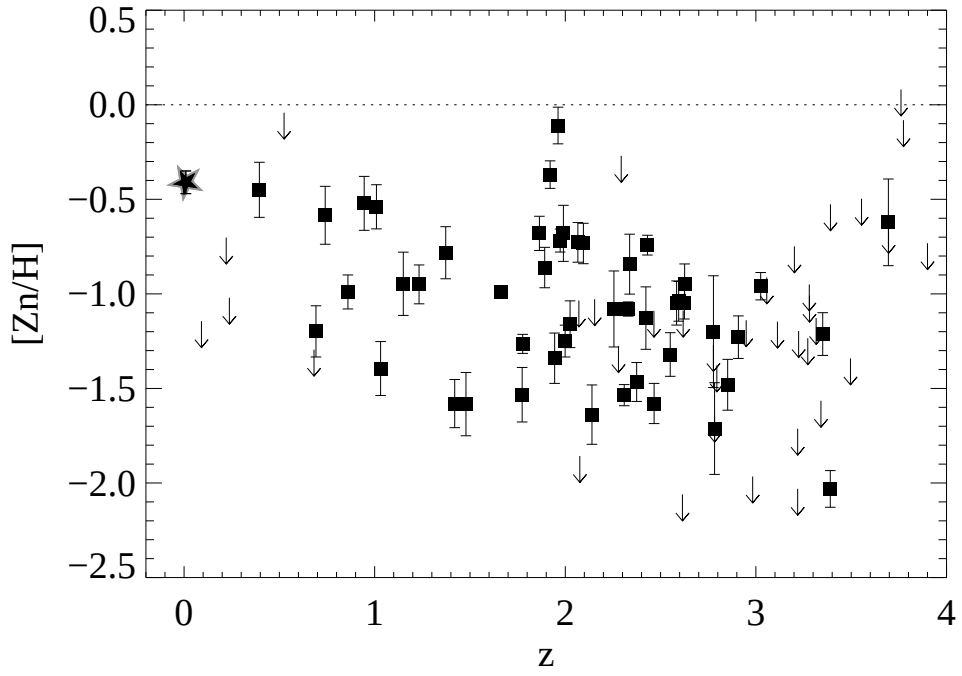

Fig. 7.— The current sample of zinc abundance measurements in DLAs, as a function of redshift z, from the compilation by Kulkarni et al. (2005). The star close to $z = 0$ represents the sulfur abundance we have measured in SBS 1543+593. Any offset between metallicities measured from zinc and sulfur is likely to be less than 0.2 dex (see Figure 9 of Nissen et al. 2004).

gas, i.e., $F_{\rm H\ II}$(C II*) in eqn (14). We can use plausible values of $Y_{n(\rm C\ II^*)}$(C II) to estimate $F_{\rm H\ II}$(C II*) via eqn 17: for the range $Y_{n(\rm C\ II^*)}$(C II) = [1,22] (see §4.2.3), we find $\log(l_c)$ = [−26.9,−25.9]. However, if the star formation rate in SBS 1543+593 is close to the value suggested in §4.2.1, $\simeq 1-2\times10^{-3}$ $M_\odot$ yr^{-1} kpc^{-2}, then: $Y_{n(\rm C\ II^*)}$(C II) must be between $\approx 1-2$; the fraction of S II which resides in ionized gas must be $<<$ 44%; the fraction of C II* arising in ionized gas would be $>$ 90 %; and the cooling rate would be close to the median value of $\log(l_c) = -27.0$ for the DLAs.

Whether such a comparison is entirely valid is, however, unclear. For the DLAs, C II* absorption is thought to come primarily from the cold *neutral* medium, i.e. with $F_{\rm H\ II}$(C II*) $\simeq$ 0 (Wolfe et al. 2004). Unfortunately, a more detailed comparison between the methods used to measure l_c in this paper and those used for the DLA population is beyond the scope of this paper.

Our observations of SBS 1543+593 provide a strong incentive for finding more examples of close QSO-galaxy pairs at low redshifts, where the galaxy producing the DLA in the QSO spectrum can be imaged and its properties measured. While on-going large scale surveys, such as the *Sloan Digital Sky Survey*, have dramatically increased the numbers of such pairs, the current lack of a sensitive, high resolution, near-UV spectrograph in space will hamper progress in this area until a worthy successor of STIS is flown.

We thank Bruce Draine for an important reading of a late draft of this paper. Support for this project was provided by NASA through grant HST-GO-09784 from the Space Telescope Science Institute, which is operated by the Association of Universities for Research in Astronomy, Inc., under NASA contract NAS5-26555. T.M.T. appreciates support from NASA grant NNG 04GG73G.

REFERENCES

Aldrovandi, S. M. V. & Pequignot, D. 1973, A&A, 25, 137

Bowen, D. V., Blades, J. C., & Pettini, M. 1995, ApJ, 448, 634

Bowen, D. V., Huchtmeier, W., Brinks, E., Tripp, T. M., & Jenkins, E. B. 2001a, A&A, 372, 820

Bowen, D. V., Tripp, T. M., & Jenkins, E. B. 2001b, AJ, 121, 1456

Bresolin, F., Garnett, D. R., & Kennicutt, R. C. 2004, ApJ, 615, 228

Cannon, J. M., Skillman, E. D., Sembach, K. R., & Bomans, D. J. 2005, ApJ, 618, 247

Chen, H.-W., Kennicutt, R. C., & Rauch, M. 2005, ApJ, 620, 703

Christensen, L., Schulte-Ladbeck, R. E., Sánchez, S. F., Becker, T., Jahnke, K., Kelz, A., Roth, M. M., & Wisotzki, L. 2005, A&A, 429, 477

de Blok, W. J. G., McGaugh, S. S., & van der Hulst, J. M. 1996, MNRAS, 283, 18

Draine, B. T. 2005, in Spitzer Space Telescope: New Views of the Cosmos, ed. L. Armus, ASP Conf. Ser. (San Francisco: Astr. Soc. Pacific), in press

Ellison, S. L., Kewley, L. J., & Mallén-Ornelas, G. 2005, MNRAS, 357, 354

Engelbracht, C. W. e. a. 2005, in Spitzer Space Telescope: New Views of the Cosmos, ASP Conf. Ser. (San Francisco: Astr. Soc. Pacific), in press

Esteban, C., Peimbert, M., García-Rojas, J., Ruiz, M. T., Peimbert, A., & Rodríguez, M. 2004, MNRAS, 355, 229

Ferland, G. J., Korista, K. T., Verner, D. A., Ferguson, J. W., Kingdon, J. B., & Verner, E. M. 1998, PASP, 110, 761

Field, G. B. & Steigman, G. 1971, ApJ, 166, 59

Fox, A. J., Savage, B. D., Wakker, B. P., Tripp, T. M., Sembach, K. R., & Bland-Hawthorn, J. 2005, ApJ, 630, 332

Fukugita, M. & Peebles, P. J. E. 2004, ApJ, 616, 643

Garnett, D. R., Edmunds, M. G., Henry, R. B. C., Pagel, B. E. J., & Skillman, E. D. 2004a, AJ, 128, 2772

Garnett, D. R., Kennicutt, R. C., & Bresolin, F. 2004b, ApJ, 607, L21

Hayes, M. A. & Nussbaumer, H. 1984, A&A, 134, 193

Horne, K. 1986, PASP, 98, 609

Howk, J. C., Wolfe, A. M., & Prochaska, J. X. 2005, ApJ, 622, L81

Jenkins, E. B. 1996, ApJ, 471, 292

Jenkins, E. B. 2004, in Carnegie Observatories Astrophysics Series, Vol. 4, Origin and Evolution of the Elements, ed. A. McWilliam & M. Rauch (Cambridge: Cambridge Univ. Press), 339

Jenkins, E. B., Gry, C., & Dupin, O. 2000, A&A, 354, 253

Jenkins, E. B. & Shaya, E. J. 1979, ApJ, 231, 55

Jenkins, E. B. & Tripp, T. M. T. 2005, ApJ, submitted

Kennicutt, R. C. 1998a, ApJ, 498, 541

—. 1998b, ARA&A, 36, 189

Kennicutt, R. C., Bresolin, F., & Garnett, D. R. 2003, ApJ, 591, 801

Kim Quijano, J. 2004, STIS Instrument Handbook, 7th edn., Space Telescope Science Institute

Kulkarni, V. P., Fall, S. M., Lauroesch, J. T., York, D. G., Welty, D. E., Khare, P., & Truran, J. W. 2005, ApJ, 618, 68

Kunth, D. & Sargent, W. L. W. 1986, ApJ, 300, 496

Lanz, T. & Hubeny, I. 2003, ApJS, 146, 417

Lehner, N., Wakker, B. P., & Savage, B. D. 2004, ApJ, 615, 767

Lodders, K. 2003, ApJ, 591, 1220

Morton, D. C. 2003, ApJS, 149, 205

Nissen, P. E., Chen, Y. Q., Asplund, M., & Pettini, M. 2004, A&A, 415, 993

Nussbaumer, H. & Storey, P. J. 1981, A&A, 96, 91

Pettini, M., Ellison, S. L., Steidel, C. C., & Bowen, D. V. 1999, ApJ, 510, 576

Prochaska, J. X., Gawiser, E., Wolfe, A. M., Castro, S., & Djorgovski, S. G. 2003, ApJ, 595, L9

Rana, N. C. 1991, ARA&A, 29, 129

Reimers, D. & Hagen, H. 1998, A&A, 329, L25

Salpeter, E. E. 1955, ApJ, 121, 161

Sarazin, C. L., Rybicki, G. B., & Flannery, B. P. 1979, ApJ, 230, 456

Savage, B. D., Drake, J. F., Budich, W., & Bohlin, R. C. 1977, ApJ, 216, 291

Savage, B. D. & Sembach, K. R. 1991, ApJ, 379, 245

—. 1996, ARA&A, 34, 279

Scalo, J. M. 1986, Fundamentals of Cosmic Physics, 11, 1

Schmidt, M. 1959, ApJ, 129, 243

Schulte-Ladbeck, R. E., König, B., Miller, C. J., Hopkins, A. M., Drozdovsky, I. O., Turnshek, D. A., & Hopp, U. 2005, ApJ, 625, L79

Schulte-Ladbeck, R. E., Rao, S. M., Drozdovsky, I. O., Turnshek, D. A., Nestor, D. B., & Pettini, M. 2004, ApJ, 600, 613

Sembach, K. R. & Savage, B. D. 1992, ApJS, 83, 147

Spitzer, L. 1978, Physical processes in the interstellar medium (New York Wiley-Interscience, 1978), p107

Spitzer, L. & Jenkins, E. B. 1975, ARA&A, 13, 133

Stasinska, G. 1990, A&AS, 83, 501

Tripp, T. M., Wakker, B. P., Jenkins, E. B., Bowers, C. W., Danks, A. C., Green, R. F., Heap, S. R., Joseph, C. L., Kaiser, M. E., Linsky, J. L., & Woodgate, B. E. 2003, AJ, 125, 3122

Tumlinson, J., Shull, J. M., Rachford, B. L., Browning, M. K., Snow, T. P., Fullerton, A. W., Jenkins, E. B., Savage, B. D., Crowther, P. A., Moos, H. W., Sembach, K. R., Sonneborn, G., & York, D. G. 2002, ApJ, 566, 857

Weingartner, J. C. & Draine, B. T. 2001a, ApJ, 563, 842

—. 2001b, ApJS, 134, 263

Wolfe, A. M. 1990, in The Interstellar Medium in Galaxies, Proceedings of the 2nd Teton Conference (Dordrecht, Netherlands, Kluwer Academic Publishers), 387

Wolfe, A. M., Gawiser, E., & Prochaska, J. X. 2003a, ApJ, 593, 235

Wolfe, A. M., Howk, J. C., Gawiser, E., Prochaska, J. X., & Lopez, S. 2004, ApJ, 615, 625

Wolfe, A. M., Prochaska, J. X., & Gawiser, E. 2003b, ApJ, 593, 215

Wolfire, M. G., Hollenbach, D., McKee, C. F., Tielens, A. G. G. M., & Bakes, E. L. O. 1995, ApJ, 443, 152